ACADEMIA ROMÂNĂ
Revue Roumaine de Chimie
http://web.icf.ro/rrch/

Rev. Roum. Chim.,
2018, *63*(5-6), 437-446

Dedicated to Dr. Maria Zaharescu
on the occasion of her 80th anniversary

THERMAL BEHAVIOUR OF SOME PRECURSORS OF ZINC ALUMINATE SPINELS USED IN A GREEN COMBUSTION METHOD

Diana VISINESCU,[a] Bogdan JURCA[b] and Oana CARP[a*]

[a] Institute of Physical Chemistry, Splaiul Independentei no.202, 060021 Bucharest, Roumania
[b] Department of Physical Chemistry, Faculty of Chemistry, University of Bucharest, Bd. Elisabeta no.12, Bucharest, Roumania

Received November 14, 2017

The thermoreactivity of five $ZnAl_2O_4$ precursors, two single-fuel and three two-fuels, was evaluated. As fuels, starch, N-methylurea and a mixture of both in different fuel/oxidant ratios were employed. The effect of fuel nature and composition on combustion behaviour was assessed.

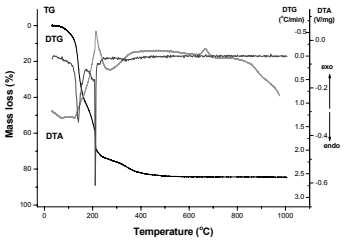

INTRODUCTION

The simultaneous thermal decomposition of a fuel (such as gluconates, citrates, urea, hydrazine, etc.) and oxidizer (such as nitrate, perchlorate, *etc*. anions) along with the redox reaction of their thermal products represents a special method to synthesize metal oxides, the so-called "combustion route".[1,2] Once initiated, the decomposition reaction is quickly propagated and the organic skeleton destroyed. The evolving of a large amount of gases leads to nanocrystalline oxides. Single[3-7] and mixed oxides such as spinel[8-10] and hexaferrites,[11-14] cobaltites,[15] aluminates,[3,16] chromites,[3,17] manganites[18,19] were obtained using this synthesis technique.

Actually, the mechanism of the combustion process in terms of the involved reactions is quite complex. The parameters which strongly influence the reactions are, mainly, the type of used fuel (F) and fuel to oxidizer (O) ratio. The traditional organic compounds used as fuels are high-temperature flame ones, mostly containing nitrogen, as urea and its derivates[20-22] and different amino acids.[6,23-25] A natural progress in the synthesis of materials is the improvement in terms of environmental impact either by (*i*) developing simple, energy and labour saving synthesis routes;[26-29] (*ii*) introducing as raw materials renewable compounds as carbohydrates, oils and fats, proteins and lignins[30-35] or, the most promising option, (*iii*) combining an efficient and economical synthesis procedure with eco-friendly raw materials.[36-39] In the case of combustion synthesis, the "greening" can be accomplished easily by a partial or total replacement of the conventional fuels with carbohydrates (biofuels).[40-45]

In combustion reactions, the carbohydrates are low-flame temperature fuels,[46] and, in a mixture with conventional high-temperature flame fuels, could

* Corresponding author email: ocarp@icf.ro

adjust the flame temperature, and, implicitly, some important characteristics of the final materials.[47-49]

Taking into account these considerations, we carried out the present study in which we analyze the influence of the fuel nature and composition on the combustion processes by means of thermal analysis. A high- and low-temperature fuel, like N-metylurea (NMU) and starch (S), respectively were used as fuels, in various NMU/S and F/O ratios.

RESULTS

Assuming a complete combustion in a system with starch and N-methylurea as fuels, for a stoichiometric F/O ratio, the theoretical equations of $ZnAl_2O_4$ formation are as following:

precursor ZA1

$$2Al(NO_3)_3{\cdot}9H_2O+Zn(NO_3)_2{\cdot}6H_2O+1.66C_6H_{10}O_5 \rightarrow ZnAl_2O_4+10CO_2+4N_2+ 32.33H_2O \quad (1)$$

precursor ZA2

$$2Al(NO_3)_3{\cdot}9H_2O+Zn(NO_3)_2{\cdot}6H_2O+3.33C_2N_2H_6O_5 \rightarrow ZnAl_2O_4+6.66CO_2+7.33N_2+33.99H_2O \quad (2)$$

precursor ZA3

$$2Al(NO_3)_3{\cdot}9H_2O+Zn(NO_3)_2{\cdot}6H_2O+0.41C_6H_{10}O_5+2.62C_2N_2H_6O_5 \rightarrow ZnAl_2O_4+7.7CO_2+6.62N_2+33.91H_2O \quad (3)$$

In the rich-fuel systems, where the quantity of oxygen is lower than the required one, for a complete combustion of the fuel, an amount of atmospheric oxygen would be needed:

precursor ZA4

$$2Al(NO_3)_3{\cdot}9H_2O+Zn(NO_3)_2{\cdot}6H_2O+3.33C_2N_2H_6O_5+0.415C_6H_{10}O_5+2.47O_2 \rightarrow ZnAl_2O_4+9.15CO_2+ +7.33N_2+36.06H_2O \quad (4)$$

precursor ZA5

$$2Al(NO_3)_3{\cdot}9H_2O+Zn(NO_3)_2{\cdot}6H_2O+3.33C_2N_2H_6O_5+0.88C_6H_{10}O_5+10.61O_2 \rightarrow ZnAl_2O_4+11.94\ CO_2+7.33N_2+ +38.39H_2O \quad (5)$$

All combustion reactions were carried out in open vessels for a good oxygen supply. The obtained oxide samples after the combustion reaction consist in pure $ZnAl_2O_4$ spinel phase.

a. Thermal behaviour of the raw materials

In order to evaluate how the used raw materials (aluminium and zinc nitrate salts, N-methylurea and starch) influence the thermoreactivity of the investigated precursors, their individual thermal behaviour is firstly presented (Figure 1).

Two decomposition stages were registered in the decomposition of $Al(NO_3)_3{\cdot}9H_2O$ (figure 1A). The first one, is a process that occurs in the temperature range 105.7-196.8°C ($T_{DTG\,max}$= 156.4°C and $T_{DTA\,min}$ = 167.7°C) and represents the evolving of the nine water molecules associated with the decomposition of one NO_3^- group[50] (mass loss exp./theor. = 60.14 / 59.18%). The second stage (196.8-522.6°C), composed of at least two overlapped processes ($T_{DTG\ max}$ = 211.6°C and ≈ 287°C, $T_{DTA\ min}$ ≈ 303° C) is assigned to the stepped evolving of the two remained nitrate groups, with the formation of Al_2O_3.

The decomposition of $Zn(NO_3)_2{\cdot}6H_2O$ takes place through three decomposition stages (figure 1B). The first stage (54.3-240.0°C T_{DTGmax} = 131.8 and 215.8°C) associated with two endothermic processes (T_{DTAmin} = 138.6 and 223.0°C) represents the six water molecules evolving (mass loss exp./theor. = 36.07/36.31%). The second and third ones are assigned to the decomposition of nitrate anions and formation of zinc oxide. During the second decomposition step (240.1-303.6°C, $T_{DTG\ max}$ = 254.7°C, $T_{DTA\ min}$ =288.5°C), 0.5 NO_3^- is decomposed (mass loss exp./theor. = 8.92/9.07%), while throughout the third one (303.6-587.4°C,

$T_{DTG\ max}$ = 317.8 and 337.6°C, $T_{DTA\ min}$ =342.1°C) the evolving of the remaining 1.5 NO_3^- occurs (mass loss exp./theor. = 27.58/27.21%).

The thermal decomposition of N-methylurea (figure 1C) starts with the melting of the organic compound ($T_{DTA\ min}$ = 107.4°C). This phase transformation is followed by two decomposition processes: the first one, in the temperature range 155.2-326.2°C, characterized by a two-stepped decomposition ($T_{DTG\ max}$ = 261.1 and 268.4°C) and a mass loss of 96.67% is associated with an endothermic effect ($T_{DTA\ min}$= 269.4°C), while the second one, up to 504.9°C, consists in a continuous constant mass loss of 3.33% coupled with two small exothermic effects ($T_{DTA\ max}$ = 410.1 and 427.7°C). The decomposition reaction takes place, most likely, *via* a (methyl)ammonium cyanate intermediate, as identified in the case of urea and alkyl-substituted urea complexes decomposition.[51,52]

Three decomposition steps are registered for starch degradation (figure 1D). The first step (49.8-175.4°C, $T_{DTG\ max}$ = 92.9°C, $T_{DTA\ min}$ = 106.9°C) is attributed to the water elimination (mass loss = 12.64%). The second step that occurs in the temperature range 244.5-394.5°C ($T_{DTG\ max}$ = 287.3°C, mass loss = 54.75%) corresponds to starch skeleton breakdown.[53] The thermal decomposition starts before starch melting as an endothermic effect at 267.9°C. An exothermic effect assigned to the starch oxidative decomposition is recorded at 303.2°C. During the next exothermic decomposition step (394.5-613.1°C, $T_{DTG\ max}$ = 509.6°C, $T_{DTA\ max}$ = 508.0°C), 31.46% of starch mass is evolved. The remaining residue (1.15%) is eliminated up to 1000°C.

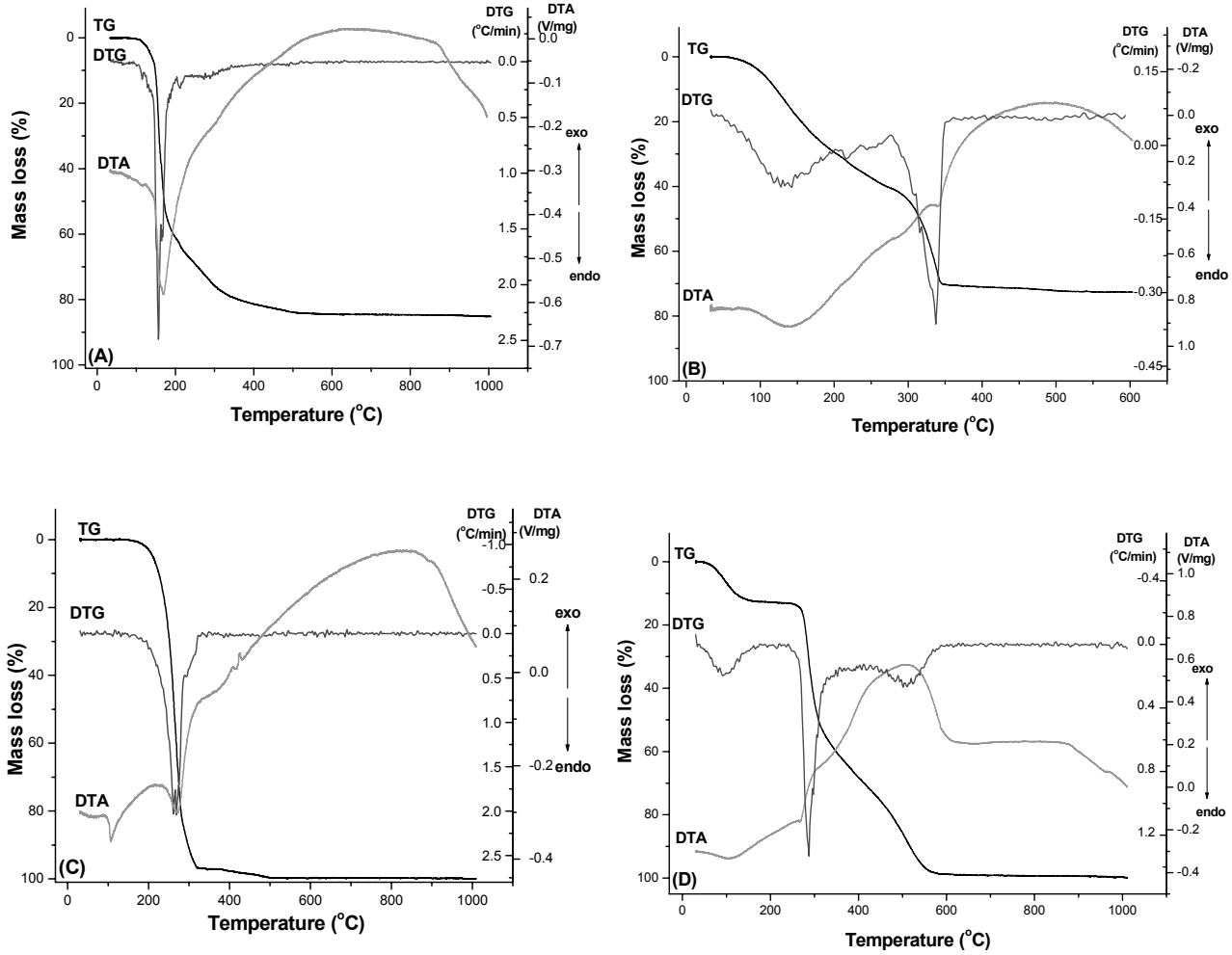

Fig. 1 – Thermal curves (TG, DTG and DTA) of (A) $Al(NO_3)_3 \cdot 9H_2O$; (B) $Zn(NO_3)_2 \cdot 6H_2O$, (C) N-methylurea and (D) starch raw material raw materials.

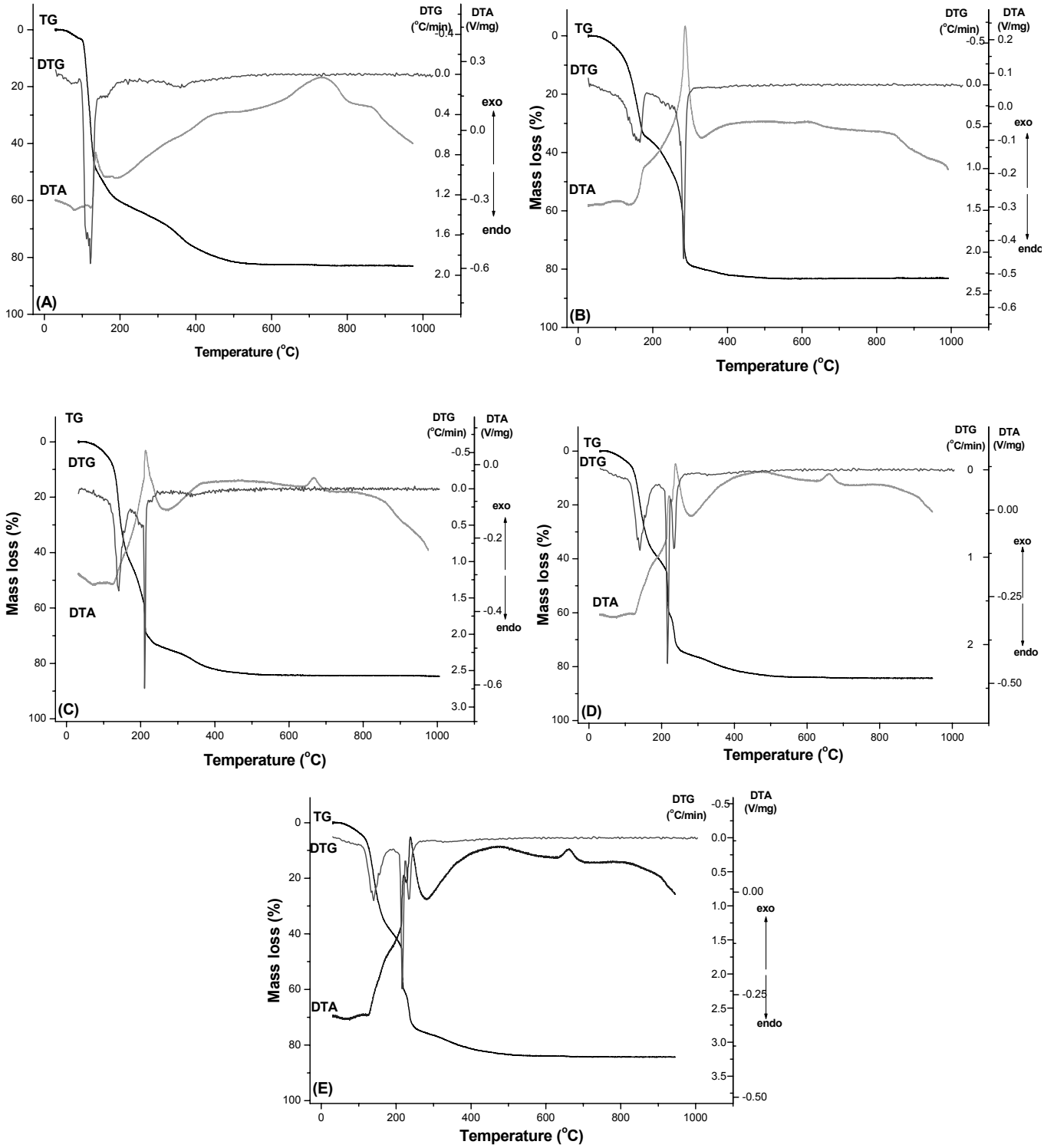

Fig. 2 – Thermal curves (TG, DTG and DTA) of $ZnAl_2O_4$ precursors: (A) ZA1; (B) ZA2; (C) ZA3; (D) ZA4 and (E) ZA5.

b. Thermal behaviour of the precursors

The thermal decomposition of the ZA1 precursor (Figure 2A, Table 1) commences with a dehydration step (50.9-91.1°C, $T_{DTG\ max}$ = 70.2°C, $T_{DTA\ min}$ = 79.2°C, mass loss = 3.05%) which is followed by a complex decomposition stage (91.9-207.9°C, $T_{DTG\ max}$ = 121.1°C mass loss = 53.3%) characterized by a first endothermic ($T_{DTA\ min}$ =121.1°C) and a second exothermic ($T_{DTA\ max}$ =136.5°C) thermal effect. Such behaviour could be explained as following: the decomposition starts

with the evolving of the nitrate anions from the aluminium nitrate (endothermic step) which triggers starch's degradation and causes a succession of redox reactions between the evolved oxidant and reductant gaseous products (exothermic step). As the temperature increases, another exothermic process occurs (207.9-593.4°C, $T_{DTG\ max}$ = 356.7°C, $T_{DTA\ max}$ = 449.8°C) characterized by a mass loss of 21.57 %. This process could be attributed to the decomposition of the remaining starch and nitrate, the characteristic absorption bands of both nitrate and fragments of starch molecules being identified in the IR spectra of the reaction intermediates isolated in this temperature range (FTIR spectra are not shown here). The exothermic effect from $T_{DTA\ max}$ = 734.2°C is ascribed to $ZnAl_2O_4$ crystallization. During the precursor decomposition, no melting point of the starch was identified.

Four decomposition stages are registered during ZA2 precursor decomposition (figure 2B). The first one (54.6-185.5°C, $T_{DTG\ max}$ = 159.1°C, mass loss = 34.82%) is characterized by two endothermic effects ($T_{DTA\ min}$ = 58.8 and 140.8°C): the former could be attributed to the evolving of the water molecules, while the second one corresponds to the partial decomposition of $Al(NO_3)_3 \cdot 9H_2O$. The melting of N-metylurea which occurs in this temperature range (*see* NMU thermal decomposition) is not identified. The second decomposition stage (185.5-314.7°C, $T_{DTG\ max}$ = 283.0°C, $T_{DTA\ max}$ = 286.4°C, mass loss = 39.08%) corresponds to the decomposition of N-methylurea and residual nitrate groups. When the temperature increases up to 428°C, a mass loss of 8.48% is registered and attributed to leftover carbonaceous oxidation. The exothermic phase transition, distinguished at $T_{DTA\ max}$ = 624.0°C, represents the crystallization of the $ZnAl_2O_4$ spinel.

The thermal curves of the ZA3-ZA5 precursors that contain both S and NMU as fuels show a similar profile (figures 2C-E). The decompositions consist in 4/5 steps of mass losses (ZA3/ZA4-ZA5) and a high-temperature exothermic phase transformation corresponding to $ZnAl_2O_4$ crystallization. As in the case of the single-fuel precursors (ZA1 and ZA2) the melting of the organic compounds is not detected.

The first decomposition stage, coupled with an endothermic effect, occurs up to a temperature of 110°C, being assigned to the water molecule elimination. The second decomposition stage, that takes place at temperatures within 200°C, starts, for all investigated precursors, with an endothermic effect which quickly is converted into an exothermic one. As in the case of ZA1 precursor, this decomposition step could be assigned to the partial degradation of aluminium nitrate, reaction that initiates the organic fuel decomposition. The next two (ZA3) or three (ZA4-ZA5) decomposition steps identified up to ~600°C represent the gradual evolving of remaining fuel and nitrate.

Comparing the obtained curves with the raw materials and single-fuel ones, we may assert that:

(i) up to 200°C, starch is the main organic compound that is degraded;

(ii) up to 290°C, during one process, for ZA3 and two for Z4-Z5 precursors, the main fuel which is decomposed is NMU;

(iii) in the temperature range 200/290 – 520/560°C, starch is main organic compound that is degraded.

It is worth to mention that the IR spectroscopy investigations showed the presence of nitrate traces in the reaction intermediates until the last decomposition step.

c. Effect of the F/O and N-metylurea/starch ratios on precursors thermal behaviour

The ZA1, ZA2 and ZA3 systems have a stoichiometric F/O ratio (equivalence ratio Φ_e = F/O = 1), while ZA4 and ZA5 are rich-fuel precursors (Φ_e equal with 1.25 respectively 1.5). The mixed-fuel systems exhibit a NMU/S ratio of 4 (ZA4, 100% NMU / 25% S), 3 (ZA3, 75% NMU / 25% S) and 2, respectively (ZA5, 100% NMU / 50% S). Based on F/O and NMU/S ratios, the following discussion can be made.

In the case of the first step, assigned to a partial NO_3^- evolving and accompanied by partial organic fuel decomposition (precursors ZA1, ZA3-5) or only a partial degradation of nitrate anion generated from aluminium nitrate (precursor ZA2), the observed $T_{DTG\ max}$ and $T_{DTA\ min}$ decrease with the increase of the starch content, the temperatures being lower in comparison with $Al(NO_3)_3 \cdot 9H_2O$ raw material. The following sequence of $T_{DTG\ max}$ and $T_{DTA\ min}$ could be written:

$$Al(NO_3)_3 \cdot 9H_2O > ZA2 > ZA4 > ZA3 > ZA5 > ZA1$$

$T_{DTG\ max}$ (°C): 167.4 > 159.1 > 141.2 > 140.8 > 137.5 > 121.1

$T_{DTA\ min}$ (°C): 167.7 > 150.8 > 123.4 ≈ 123.4 > 123.4 > 122.9

Table 1

Thermoanalytical data of the four raw materials and five precursors of $ZnAl_2O_4$ (heating rate 10°C min^{-1})

Sample	Process	T_i^1-T_f^2 (°C)	$T_{max\ DTG}^3$ (°C)	$T_{max/min\ DTA}^4$ (°C)	ΔH	Δm (%)	Observations
$Al(NO_3)_3 \cdot 9H_2O$	1.	105.7-196.8	156.4	167.7	endo	59.18	-9 H_2O
			167.4				1 NO_3^- degradation
	2.	196.8-522.6	211.6	≈303	endo	22.05	2 NO_3^- degradation
			≈287			13.94	
$Zn(NO_3)_2 \cdot 6H_2O$	1.	54.3-240.0	131.8	138.6	endo	36.07	-6 H_2O
			215.8	223.0	endo		
	2.	240.0-303.6	254.7	288.5	endo	8.92	
	3.	303.68-362.0	317.8	342.2	exo	25.2	
			338.16				
	4.	362.6-587.45		≈482	exo	1.49	
$(C_6H_{10}O_5)_n$	1.	49.8-175.4	92.9	106.9	endo	12.64	dehydration
	2.	244.5-394.5	287.3	267.9	endo	54.75	melting
				303.2	exo		oxidative degradation of S
	3.	394.5-613.1	509.6	508.6	394.5	31.46	oxidative degradation of S
	4.	613.1-1000				1.15	carbonaceous reside
$CH_3NHCONH_2$	1.			107.4			melting
	2.	155.2-326.2	261.1	269.4	endo	96.67	NMU degradation
			268.4				
	3.	326.2-499.0		410.1	exo	3.33	carbonaceous reside evolving
				424.7	exo		
ZA1	1.	50.9-91.1	70.2	79.2	endo	3.05	dehydration
	2.	91.9-207.9	121.1	122.9	endo	58.3	NO_3^- and S degradation
				136.5	exo		
	3.	207.9-593.4	356.7	449.8	exo	21.57	NO_3^- and S degradation
	4.	577.0-818.2		734.4	exo	phase transition	$ZnAl_2O_4$ crystallization
ZA2	1.	54.6-185.5	159.1	58.8	endo	34.82	H_2O evolving NO_3^- degradation
				140.8	endo		
	2.	185.5-314.7	283.0	286.4	exo	39.08	NO_3^- and NMU degradation
	3.	314.7-428.8		≈366	≈388	8.48	carbonaceous reside evolving
	4.	586.5-663.6		≈618	exo		$ZnAl_2O_4$ crystallization

Table 1 (continued)

ZA3	1.	52.7-99.87		69.5	endo	2.57	dehydration
	2.	99.8-172.3		123.4	endo→ exo	40.5	NO_3^- and F degradation
	3.	172.3-259.9	210.6	214.2	exo	30.83	
	4.	259.9-506.5	337.3	355.0	exo	10.14	
	5.	632.0-706.1		667.4	exo	phase transition	$ZnAl_2O_4$ crystallization
ZA4	1.	54.3-106.6		64.52	endo	3.94	dehydration
	2.	106.6-109.8	141.20	124.5	endo→ exo	35.67	NO_3^- and F degradation
	3.	109.8-280.1	216.95	220.6	exo	21.98	
	4.	224.4-280.1	235.48	238.7	exo	13.92	
	5.	280.1-497.4	338.3	360.8	exo	22.21	
	6.	625.6-705.0		660.1	exo	phase transition	$ZnAl_2O_4$ crystallization
ZA5	1.	49.8-111.0		66.81	endo	3.93	dehydration
	2.	111.0-179.9	137.5	123.4	endo→ exo	40.06	NO_3^- and F degradation
	3.	179.9-213.1	209.8	207.3	exo	21.4	
	4.	213.1-252.2	221.5	220.3	exo	10.14	
	5.	252.2-560.0	352.7	374.2	exo	9.66	
	6.	622.9-799		704.9	exo	phase transition	$ZnAl_2O_4$ crystallization

T_i[1] = initial temperature of descomposition; T_f[2] = final temperature of reaction; $T_{max\ DTG}$[3] = temperatura maxima DTG; $T_{max\ DTA}$[4] = temperatura maxima DTA

Thus, the precursor system containing only NMU (ZA2) presents the highest temperatures of the transformation, while the lowest temperatures is achieved for the precursor containing only starch (ZA1).

The presence of starch determines an interesting evolution of the endothermic decomposition process of NMU (ZA3-ZA5) that takes place up to 290°C. If NMU single-fuel precursor (ZA2) exhibits only one decomposition step, with $T_{DTG\ max}$ and T_{DTA} shifted towards higher temperatures in comparison with pristine NMU as a consequence of N-methylurea coordination (knowning that the coordinated ligand decomposes at higher temperature comparative with the free one[54,55]), in the mixed-fuels systems the $T_{DTG\ max}$ and T_{DTA} temperatures are lower comparative with NMU corresponding temperature. A decrease of these temperatures with the increase of starch content is identified. A higher equivalence ratio Φ_e due to a starch excess, leads to an increase of the decomposition steps and, implicitly, of the reaction stoichiometry: ZA3 precursor (75% NMU + 25% S, $\Phi_e = 1$) decomposes through a single step, while ZA4 (100% NMU + 25% S, $\Phi_e = 1.25$) and ZA5 (100% NMU + 50% S, $\Phi_e = 1.5$) precursors present a two-stepped decomposition, similar to this corresponding to free NMU. Such behaviour may be induced by a preferential coordination to the metal cations to starch, NMU acting more like a free (uncoordinated) compound. Considering only the first decomposition step of this temperature range, the order of the $T_{DTG\ max}$ and T_{DTA} temperatures is:

ZA2 > NMU > ZA4 > ZA3 > ZA5
$T_{DTG\ max}$ (°C): 283.0 > 261.1 > 216.9 > 2 10.6 > 207.3
T_{DTA} (°C): 286.4 > 269.4 > 220.6 > 214.2 > 207.3

The characteristic temperatures of the final decomposition stage, assigned mainly to the starch and nitrate decomposition, increase with the increase of starch content, the main variation being registered when NMU (between ZA1/ZA5) is added:

ZA1 > ZA5 > ZA3 > ZA4
T_f (°C): 593.4 > 564.0 > 506.5 > 497.4
$T_{DTG\ max}$ (°C): 356.7 > 352.7 > 339.0 ≈ 338.3
$T_{DTA\ max}$ (°C): 449.8 > 374.2 > 361.0 ≈ 360.8

The same order is obtaind for the characteristics temperatures (T_i, T_f, and $T_{DTA\ max}$) of the phase transition assigned to $ZnAl_2O_4$ spinel crystallization:

ZA1 > ZA5 > ZA3 > ZA4 >ZA2
T_i (°C): 577.0 >622.90 >623.3 ≈625.6 >586.5
T_f (°C): 818.3 >799.0 > 706.1 ≈705.0 >663.6
$T_{DTA\ max}$ (°C): 734.4 > 704.9 > 667.4 > 660.1 ≈ 618.4

The decrease of the final temperature is 155°C between ZA2 (only NMU) and ZA1 (only starch). Major variations of the temperature are observed when NMU/S ratio varies from 3 to 2 (93°C, between ZA3/ZA5) and when starch is eliminated from the fuel composition (41°C, between ZA4/ZA2). The results are linked with the flame temperature of the used fuels: a higher flame temperature (higher NMU content) induces a partial crystallization of the spinel oxides simultaneously with the precursor degradation.

The temperature at which the oxides are obtained influences many characteristics of the oxides like crystallinity, lattice defects, surface area and porosity, etc, which, in turn, dictates important properties such as optical, magnetical, catalytical ones. Without going into details, for the oxides generated from stoichiometric F/O ratio precursors ($\Phi_e = 1$, ZA1-ZA3), the found particle sizes and specific surfaces are dependent on registered temperatures. The dependence is not valid for oxides derived from rich-fuel precursors ($\Phi_e = 1.25$ and 1.5, ZA4 and ZA5, respectively), due to the presence undecomposed carbonaceous residues on the oxide of surface.

EXPERIMENTAL

The synthesis of the $ZnAl_2O_4$ precursors was performed using a solid state method. The starting materials of analytical grade, $Al(NO_3)_3{\cdot}9H_2O$ (Merck), $Zn(NO_3)_3{\cdot}6H_2O$ (Merck), N-methylurea ($CH_3NHCONH_2$, Merck) and starch $(C_6H_{10}O_5)_n$,

(Reactivul) were used without any further purification. The utilized molar ratios for $Zn(NO_3)_2 \cdot 6H_2O$ - $Al(NO_3)_3 \cdot 9H_2O$ – starch (anhydrous) - methylurea system were 1:2:1.66:0 (ZA1), 1:2:0:3.33 (ZA2), 1:2:0.41:2.62 (ZA3), 1:2:0.41:3.33 (ZA4), and 1:2:0.83:3.33 (ZA5). The compositions were selected in order to obtain stoichiometrical (ZA1-ZA3) and fuel rich precursors systems (ZA4-ZA5). The oxidant/fuel stoichiometry is calculated by using the oxidizing valence of metal nitrates (oxidant) and the reducing valence of starch and N-methylurea (fuels).[56] The raw materials are mixed about ~ 30 minutes in an agate pestle, in order to obtain homogenous slurry. The homogenization is followed by a drying over P_2O_5. In order to obtain the spinel oxides, the precursors were subjected to a heating treatment of one hour at 800°C. Thermal measurements were performed on a Q-1500 Paulik- Paulik-Erdey derivatograph, in static air, with a heating rate of 10°C/min and a sample mass of ~20 mg.

CONCLUSIONS

The present study demonstrates that the combustion synthesis can be simply modulated by using a mixture of fuels, with different flame-temperatures, in diverse proportions. The thermoreactivity of the five investigated precursors proves that the nature and composition of the fuel drastically influence the progress of the combustion. In our particular case, the introduction of starch as co-fuel together with N-methylurea, mitigates the N-methylurea-nitrate vigorous and explosive combustion: all the characteristic temperatures of the degradation and phase transformation (crystallization of the $ZnAl_2O_4$ spinel) processes increasing with starch content increment. As a consequence, the properties of the final oxides, related to the synthesis temperature, are adjusted.

REFERENCES

1. S. R. Jain, K. C. Adiga and V. Pai Verneker, *Combust. Flame*, **1981**, *40*, 71-79.
2. O. Carp, L. Patron and A. Reller, *Rev. Roum. Chim.*, **2002**, *48*, 513-520.
3. A. S. Prakash, A. M. A. Khadar, K. C. Patil and M. S. Hedge, *J. Mater. Synt. Proc.*, **2002**, *10*, 135-141.
4. O. Carp, L. Patron and A. Reller, *J. Therm. Anal. Calorim.*, **2003,** *73*, 867-876.
5. T. Mokkelbost, I. Kaus, T. Grande and M.-A. Einarsrud, *Chem. Mater.*, **2004,** *16,* 5489-5494.
6. O. Carp, L. Patron, L. Diamandescu, A. Reller, *Thermochim. Acta*, **2002,** *390*, 169-177.
7. K. Hembram, D. Sivaprahasam and T. N. Rao, *J. Eur. Ceram. Soc.*, **2011**, *31*, 1905-1913.
8. D. Gingasu, I. Mindru, L. Patron, O. Carp, D. Matei, C. Neagoe and I. Balint, *J. Alloys Compd.*, **2006**, *425*, 357-361.
9. A. B. Salunkhe, V. M. Khot, M. R. Phadatare, N. D. Thorat, R. S. Joshi, H. M. Yadav and S. H. Pawar, *J. Magn. Magn. Mater.*, **2014**, *352*, 91–98.
10. O. Carp, L. Patron and A. Reller, *Mat. Chem. Phys.*, **2007**, *101*, 142-147.
11. L. Junliang, Z. Wei, G. Cuijing and Z. Yanwei, *J. Alloys Compd.*, **2009**, *479*, 863-869.
12. N. J. Shirtcliffe, S. Thompson, E. S. O'Keefe, S. Appleton and C. C. Perry, *Mater. Res. Bull.*, **2007**, *42*, 281-287.
13. O. Carp, L. Patron, I. Mindru and M. Brezeanu, *Rev. Roum. Chim.*, **2002**, *47*, 969-972.
14. R. Ezhil Vizhi, V. Harikrishnan, P. Saravanan and D. Rajan Babu, *J. Cryst. Growth*, **2016**, *452*, 117–124.
15. N. P. Bansal and Z. Zhong, *J. Power Sources*, **2006**, *158*, 148–153.
16. K. Prabhakaran, D. S. Patil, R. Dayal, N. M. Gokhale and S. C. Sharma, *Mater. Res. Bull.*, **2009**, *44*, 613–618.
17. P. S. Sathiskumar, C. R. Thomas and G. Madras, *Ind. Eng. Chem. Res.*, **2012,** *51*, 10108-10116.
18. D. P. Tarragó, C. de Fraga Malfatti and V. C. de Sousa, *Powder Technol.*, **2015**, *269*, 481-487.
19. P. Manikandan, M. V. Ananth, T. Prem Kumar, M. Raju, P. Periasamy and K. Manimaran, *J. Power Sources*, **2011**, *196*, 10148-10155.
20. O. Carp, L. Patron and M. Brezeanu. *J. Therm. Anal. Cal.*, **1999**, *56*, 561-568.
21. A. Manikandan, L. J. Kennedy, M. Bououdina and J. J. Vijaya, *J. Magn. Magn. Mater.*, **2014**, *349*, 249–258.
22. B. Jurca, C. Paraschiv, A. Ianculescu and O. Carp, *J. Therm. Anal.Calorim*., **2009**, *97*, 91-98.
23. C. Paraschiv, B. Jurca, A. Ianculescu and O. Carp, *J. Therm. Anal. Calorim.*, **2008**, *94*, 411-416.
24. S. T. Aruna, N. S. Kini and K. S. Rajam, *Mater. Res. Bull.,* **2009**, *44*, 728–733.
25. J. Yang, X. Li, J. Zhou, Y. Tang, Y. Zhang and Y. Li, *J. Alloys Compds.*, **2011**, *509*, 9271– 9277.
26. O. Carp, A. Tirsoaga, R. Ene, A. Ianculescu, R. F. Negrea, P. Chesler, G. Ionita and R. Birjega, *Ultrason. Sonochem.*, **2017**, *36*, 326-335.
27. G. Patrinoiu, J. M. Calderon-Moreno, D. C. Culita, R. Birjega, R. Ene and O. Carp, *Solid State Sci.*, **2013**, *23*, 58-64.
28. Y. Mao, T.-J. Park, F. Zhang, H. Zhou and S. S. Wong, *Small*, **2007**, *3*, 1122 – 1139.
29. K. Liu and L. Jiang, *Nano Today,* **2011**, *6*, 155-175.
30. O. Carp, A. Tirsoaga, B. Jurca, R. Ene, S. Somacescu and A. Ianculescu, *Carbohydr. Polym.*, **2015**, *115*, 285-293.
31. L. Mortain, I. Dez and P.-J. Madec, *C. R. Chimie*, **2004**, *7*, 635–640.
32. A. M. Musuc, R. Dumitru, A. Stan, C. Munteanu, R. Birjega and O. Carp, *J. Therm. Anal. Calorim.*, **2015**, *120*, 85-94.
33. J. O. Metzger and M. Eissen, *C. R. Chimie*, **2004***, 7*, 569–581.
34. D. Visinescu, G. Patrinoiu, A. Tirsoaga and O. Carp, in "Environmental Chemistry for a sustainable World", ed. E. Lichtfouse, J. Schwarbauer and D. Roberts, Springer, **2012**, p. 119–172.
35. O. Carp, L. Patron, D. Culita, P. Budrugeac, M. Feder and L.Diamandescu, *J. Therm. Anal.Calorim*., **2010**, *101*, 181-187.
36. A. Stan, C. Munteanu, A. M. Musuc, R. Birjega, R. Ene, A. Ianculescu, I. Raut, L. Jecu, M. Badea Doni, E. M. Anghel and O. Carp, *Dalton Trans.*, **2015**, *44*, 7844-7853.
37. M.-M. Titirici and M. Antonietti, *Chem. Soc. Rev.,* **2010**, *39*, 103–116.

38. G. Patranoiu, J. M. Calderon-Moreno, C. M. Chifiriuc, C. Saviuc, R. Barjega and O. Carp, *J. Colloid. Interf. Sci.,* **2016**, *462*, 64-74.
39. O. Carp, D. Visinescu, G. Patrinoiu, A. Tirsoaga, C. Paraschiv and M. Tudose, *Rev. Roum. Chim.*, **2010**, *55,* 705-709.
40. A. S. Mukasyan and P. Dinka, *Adv. Eng. Mater.*, **2007**, *9*, 653-657.
41. D. Visinescu, A. Tirsoaga, G. Patrinoiu, M. Tudose, C. Paraschiv, A. Ianculescu and O. Carp, *Rev. Roum. Chim.*, **2010**, *55*, 1017-1026.
42. W. Zhou, Z. Shao, R. Ran, H. Gu, W. Jin and N. Xu, *J. Am. Ceram. Soc.*, **2008**, *91*, 1155-1162.
43. D. Visinescu, F. Papa, A.C. Ianculescu, I. Balint and O. Carp, *J. Nanopart. Res.*, **2013**, *15*, art. no. 1456.
44. J. M. Amarilla, R. M. Rojas and J. M. Rojo, *J. Power Sources,* **2011**, *196,* 5951-5959.
45. Y. Cai, H. Fan, M. Xu and Q. Li, *Colloids Surf. A*, **2013***, 436,* 787-795.
46. A. Tirsoaga, D. Visinescu, B. Jurca, A. Ianculescu and O. Carp, *J. Nanopart. Res.*, **2011**, *13*, 6397-6408.
47. K. Tahmasebi and M. H. Paydar, *Mater. Chem. Phys*., **2008**, *109*, 156-163.
48. D. Visinescu, B. Jurca, A. Ianculescu and O. Carp, *Polyhedron*, **2011**, *30*, 2824-2831.
49. C.-G. Han, C. Zhu, G. Saito and T. Akiyama, *Adv. Powder Technol.*, **2015**, *26*, 665-671.
50. Y. Zhang and G. Stangle, *J. Mater. Res.*, **1994**, *9*, 1997-2004.
51. B. Pacewska and M. Keskr, *Thermochim. Acta*, **2002**, *385*, 73-80.
52. O. Carp, *Rev. Roum. Chim.,* **2001,** *46*, 735-740.
53. A. M. Barrios and S. J. Lippard, *Inorg Chem.*, **2001**, *40*, 1250-1255.
54. B. Jurca, A. Tirsoaga, A. Ianculescu and O. Carp, *J. Therm. Anal. Calorim.*, **2014**, *115*, 495-501.
55. S. B. Jagtap, R. C. Chikate, O. S. Yemul, R. S. Ghadage and B. A. Kulkarni, *J. Therm. Anal. Cal.*, **2004**, *78*, 251-262.
56. O. Carp in "Reaction and mechanism in termal Analysis of Advanced materials", A. Tiwari and B. Raj (Eds.), Wiley, 2015, p. 63-84.